

Small-Angle Scattering Investigations of Poly(ϵ -caprolactone)/Polycarbonate Blends. 1. Small-Angle Neutron and X-ray Scattering Study of Crystalline Blend Morphology

Y. Wilson Cheung* and Richard S. Stein*

Department of Polymer Science and Engineering, University of Massachusetts, Amherst, Massachusetts 01003

George D. Wignall

Oak Ridge National Laboratory, Oak Ridge, Tennessee 37830

Hsinjin E. Yang

Eastman Kodak Company, Rochester, New York 14650

Received May 21, 1993; Revised Manuscript Received July 12, 1993*

ABSTRACT: Crystalline morphologies of poly(ϵ -caprolactone) (PCL) and deuterated polycarbonate (d-PC) blends were studied by small-angle neutron and X-ray scattering (SANS and SAXS). Measurements were conducted at both room temperature and temperatures above the melting point (60 °C) of PCL. Due to the different contrast between the phases for neutrons and X-rays, SANS exhibited a monotonic drop in intensity with increasing scattering angle while SAXS showed lamellar (peak) scattering. A two-correlation length model provided an excellent fit for the SANS data over the entire composition range. This model reproduced not only the shape but also the absolute magnitude of the scattering curves. The long range correlation length ($\sim 10^2$ Å) and the short range correlation length (~ 10 Å) derived from this model are inferred to be associated with the crystalline PC domain and the local cluster in the amorphous phase (possibly resulting from crystallization-induced phase separation), respectively. Both the long range correlation length obtained from SANS and the long period measured from SAXS showed identical composition dependence. This further supports the applicability of the two-correlation length model and our interpretation.

Introduction

Blending of two or more polymers is a very cost effective way of producing new materials with tailor-made properties.¹ A thorough understanding of both the thermodynamic and kinetic forces controlling the blend structure and thus its properties is indispensable for engineering useful materials. Blends of poly(ϵ -caprolactone) (PCL) and polycarbonate (PC) are miscible in the amorphous phase over the entire composition range, as revealed by differential scanning calorimetry (DSC) and dynamic mechanical analysis (DMA).² The phase behavior of this system is extremely complicated and enormously rich.³ PC is normally classified as an amorphous polymer. Interestingly, upon mixing PC with PCL, PC can readily undergo crystallization even at room temperature. Additionally, the PCL/PC blends exhibit a lower critical solution temperature (LCST at about 260 °C) where demixing occurs at temperatures close to the degradation temperatures. Depending on the composition and temperature, the PCL/PC blend system could be semicrystalline/semicrystalline, semicrystalline/amorphous, amorphous/amorphous, and immiscible. Both the phase behavior of the blends and the PCL crystallization kinetics in the semicrystalline/semicrystalline state will be reported in the forthcoming publications.⁴ The focus of this series of papers is to quantify miscibility in the amorphous state and to elucidate the crystalline blend morphologies in both the semicrystalline/semicrystalline and semicrystalline/amorphous state. A detailed presentation of the small-angle X-ray (SAXS) results on both hydrogenated PC (h-PC)/PCL and deuterated PC (d-PC)/PCL blends including the correlation function analysis and invariant calculation will be reported in a separate communication.⁵ Attention

will be directed at a critical analysis of the small-angle neutron scattering (SANS) results of d-PC/PCL blends in the present paper.

Small-angle neutron scattering (SANS) is a powerful technique for probing polymer blend morphology.⁶ In most SANS studies of polymer blends, one component is normally deuterated and the other is hydrogenated to create scattering contrast. It has been observed that deuteration may perturb the thermodynamics of the system.⁷ Therefore, it is important to stress the results derived from this study may not truly reflect the behavior of the corresponding hydrogenated system. Application of SANS and SAXS for studying polymer blend morphology has been demonstrated to be highly effective in yielding unambiguous structural information.^{6,8} This synergism comes about because the contrast mechanism in SAXS is very different from that of SANS. SAXS arises from the difference in electron density difference (e.g. amorphous and crystalline region), whereas SANS arises from scattering length density (SLD) differences. The latter are dominated by the substitution of deuterium for hydrogen, due to the change of sign in the scattering length ($b_D = 0.667 \times 10^{-12}$ cm; $b_H = -0.374 \times 10^{-12}$ cm). Since PC is deuterated in the work reported here, SANS directly probes the spatial arrangement between PC and PCL whereas SAXS probes the amorphous/crystalline region.

Experimental Section

The deuterated PC was synthesized by solution polymerization of deuterated Bisphenol with phosgene at 0 °C in methylene chloride. Pyridine was used to neutralize the hydrochloric acid generated from the condensation reaction. The resulting polymer was then washed in water and precipitated out of methanol. Both PCL and h-PC were obtained from Scientific Polymer Products. The molecular weights of d-PC, h-PC, and PCL, determined from gel permeation chromatography, are shown in Table I. Blends were prepared by dissolving the two components in

* Abstract published in *Advance ACS Abstracts*, September 1, 1993.

Table I. Molecular Weights for Poly(ϵ -caprolactone) (PCL), Hydrogenous Polycarbonate (h-PC), and Deuterated Polycarbonate (d-PC)

polymer	M_w	M_n	M_w/M_n
PCL	23 700	16 500	1.44
h-PC	23 100	36 400	1.57
d-PC	134 000	15 600	8.6

methylene chloride. The blend solution was then cast on an aluminum surface. The sample was first dried under ambient conditions overnight and then was vacuum dried at 90 °C for 2 days to ensure complete removal of residual solvent. Crystalline h-PC was also prepared in a manner identical with that of the blends where PC crystallinity was enhanced by means of solution-induced crystallization. Scattering samples were compression molded typically at $T_g + 50$ °C under vacuum. Samples were then rapidly transferred to a metal surface and quenched to room temperature. Sample disk dimension was about 1 mm in thickness and 15 mm in diameter.

Thermal transitions of the blends were measured with a DuPont-10 differential scanning calorimeter (DSC) at a heating rate of 20 °C/min. The glass transition temperatures were obtained from the second heating scan and determined from the midpoint of the change in heat capacity. The melting endotherms of both components were recorded from the first heating scan. On the basis of the values of the heat of fusion for 100% crystalline PC⁹ (35.3 cal/g) and PCL¹⁰ (32.4 cal/g), the degree of crystallinity of both PC and PCL was calculated from the melting endotherm and normalized with respect to the composition of each component in the blend.

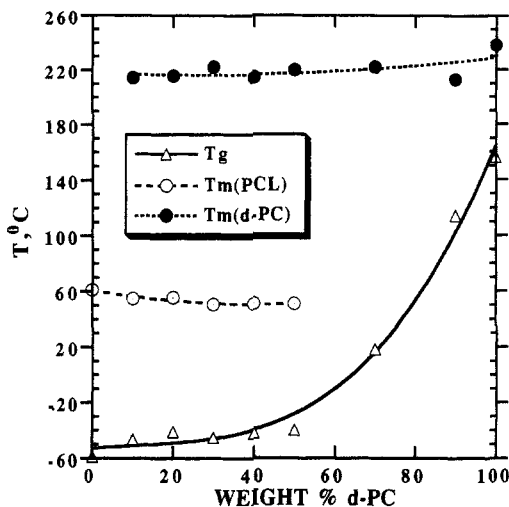
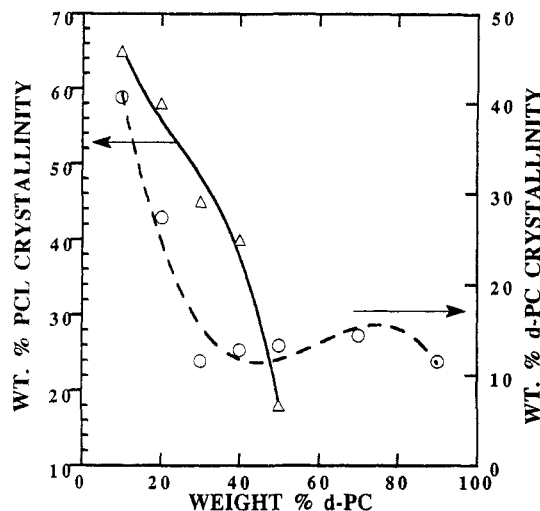
Both SANS and SAXS measurements were performed at Oak Ridge National Laboratory (ORNL) in Tennessee. SANS experiments were conducted on the W. C. Koehler 30-m spectrometer. The neutron wavelength was 4.75 Å ($\Delta\lambda/\lambda = 5\%$) and the source (3.5-cm diameter) and sample (1.0-cm-diameter) slits were separated by a distance of 7.5 m. The sample-detector distance was 10 m, and the data were corrected for instrumental backgrounds and detector efficiency on a cell-by-cell basis, prior to radial averaging to give a q range of 0.007–0.07 Å⁻¹. The net intensities were converted to an absolute ($\pm 5\%$) differential cross section per unit sample volume (in units of cm⁻¹) by comparison with precalibrated secondary standards.¹¹ Incoherent scattering backgrounds were estimated from the scattering of the hydrogenous polymers and were subtracted from the sample scattering.

The transmission of the sample was measured in a separate experiment¹² by collimating the beam with slits (irises) ~1 cm in diameter, separated by ~7.5 m. A strongly scattering sample, porous carbon, was placed at the sample position to spread the beam over the whole detector, positioned at a sample-detector distance ~10 m. The total count summed over the whole detector ($>10^5$) was recorded in a time period ~1 min and the sample being measured was placed over the source slit, thus attenuating the beam. The count was repeated over the same time interval, and the transmission was given by the ratio of the two counts after minor corrections ($<0.1\%$) for the beam-blocked background due to electronic noise, cosmic rays, etc.

SAXS measurements were performed on the ORNL 10-m spectrometer¹³ operating at an accelerating voltage of 40 keV and a current of 100 mA. The instrument was operated with a sample-detector distance of 5.17 m using Cu K α radiation ($\lambda = 1.54$ Å) and a 20 × 20-cm² area detector with cell (element) size ~3 mm. Corrections were made for instrumental backgrounds and detector efficiency (via an Fe⁵⁵ standard which emits γ -rays isotropically) on a cell-by-cell basis, prior to radial averaging to yield a q range of 0.005–0.1 Å⁻¹. As in the SANS experiments, the net scattering intensities were converted to an absolute differential cross section by means of precalibrated secondary standards.¹⁴

Experimental Results

Differential Scanning Calorimetry. In agreement with previous studies, d-PC appears to be miscible with PCL in the amorphous phase over the entire composition range, as evidenced by the presence of a single glass

**Figure 1.** Thermal transitions for d-PC/PCL blends.**Figure 2.** Normalized PCL and d-PC crystallinities (for solution cast samples) for d-PC/PCL blends.

transition temperature shown in Figure 1. For blends containing more than 50% PCL,⁴ both PCL and d-PC crystallize readily at room temperature (RT), as indicated by the presence of two distinct melting transitions. Hence, these materials are semicrystalline/semicrystalline. At temperatures above the melting point (60 °C) of PCL, the PCL rich blends become semicrystalline/amorphous. Normally, d-PC in the d-PC rich blends cannot crystallize at RT. Since the samples were prepared from solution casting, even d-PC rich blends are semicrystalline/amorphous at RT due to solution-induced crystallization. Due to the presence of crystallinities, the composition of the amorphous phase is different from the overall blend composition. Thus, the measured T_g shown in Figure 1 only reflects that of the semicrystalline samples, as truly amorphous samples cannot be prepared due to the thermodynamics of the system. This complication will be addressed in a later communication.⁴ Both the PCL and d-PC crystallinities (for the solution cast samples), normalized with respect to the composition of each component, as a function of composition are plotted in Figure 2. The PCL crystallinity decreases with increasing d-PC concentration, whereas the d-PC crystallinity exhibits a much more complex composition dependence.

The effects of sample preparation and thermal history on the degree of crystallinity were also investigated and will be reported in a forthcoming communication.⁴ It is found that the PCL crystallinity is higher for the solution cast samples than that obtained for the precipitated

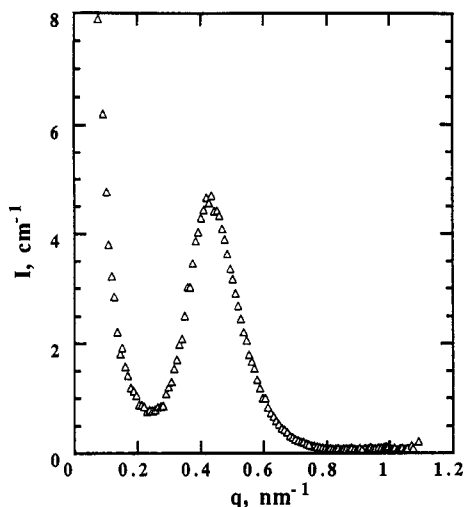


Figure 3. SAXS for PCL recorded at room temperature.

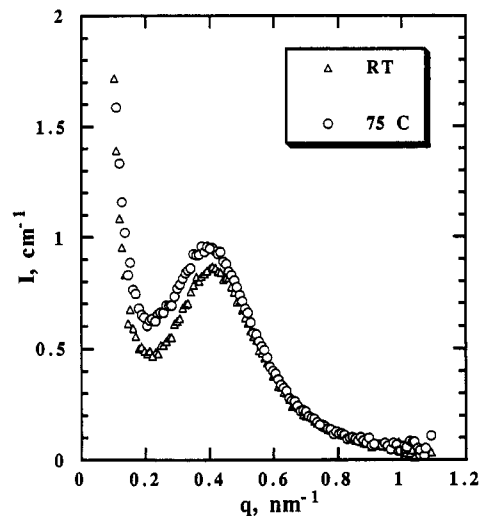


Figure 4. SAXS for homogeneous (crystalline) PC.

(blends recovered from precipitation in methanol) samples where solution-induced crystallization was greatly suppressed. Moreover, the PCL crystallinity for the precipitated samples crystallized either isothermally or athermally undergoes a significant reduction at about 30% PC composition. Similar to the solution cast samples, the h-PC crystallinity for the precipitated blends also exhibits a nonmonotonic composition dependence.

Contrast Variations. Before embarking on the discussion of the scattering profiles of the blends, the SANS and SAXS profiles of the two homopolymers should be examined. The SAXS plots for PCL and PC are shown in Figure 3 and 4, respectively. The SAXS and SANS profiles for PC recorded at RT and elevated temperatures are almost identical. The SAXS clearly shows strong lamellar scattering, whereas the SANS plot is essentially flat and appears to be dominated by incoherent scattering. In contrast, a peak should emerge in the SANS for a 100% deuterated semicrystalline PC, due to the positive and negative scattering lengths of D^2 and H^1 , as such a sample is not available for this study. Similarly, PCL shows the same scattering behavior as the PC where the SANS appears virtually flat and is predominantly comprised of the incoherent component.

Figure 5 shows a typical SANS plot for a 50% d-PC/50% PCL blend recorded at both RT and 85 °C. The scattering profiles at RT and 85 °C are almost superimposable for all the blends, thus indicating that the SANS is invariant with respect to the physical state (amorphous

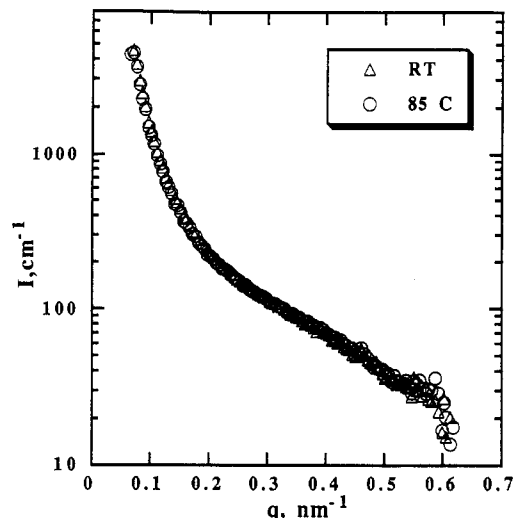


Figure 5. SANS for a 50% d-PC/50% PCL blend.

Table II. Neutron Scattering Length Density (SLD), Electron Density (ρ_e), and Mass Density (d) for PCL, h-PC, and d-PC

polymer	$10^{-8}\text{SLD, cm}^{-2}$	$10^{-9}\rho_e, \text{cm}^{-2}$	$d_A, \text{g/cm}^3$	$d_X, \text{g/cm}^3$
PCL	7.37d	91.72d	1.090	1.185
h-PC	16.75d	88.97d	1.196	1.315
d-PC	51.21d	88.97d	1.196	1.315

Table III. Neutron Scattering Length Density Difference (DSLD) and Electron Density Difference ($\Delta\rho_e$) for Various Components

component ^a	$10^{-20}(\Delta\text{SLD})^2, \text{cm}^{-4}$	$10^{-20}(\Delta\rho_e)^2, \text{cm}^{-4}$
d-PC _A /PCL _A	28.319	
d-PC _A /PCL _X	27.579	
dPC _X /PCL _A	35.177	
d-PC _X /(PCL _A + d-PC _A)	0.0375	
d-PC _X /d-PC _A	0.371	
h-PC _X /h-PC _A	0.0397	1.118
PCL _X /PCL _A	0.00490	0.760

^a A = amorphous, X = crystalline.

or crystalline) of PCL. Furthermore, the intensity for all the SANS plots decreases monotonically with the scattering vector q . These two findings suggest that the SANS is dominated by the contrast between d-PC and PCL. The neutron scattering length density (SLD), electron density and the mass density for h-PC, d-PC, and PCL are shown in Table II. On the basis of the contrast comparisons shown in Table III, the absence or the "smearing" of the PCL and PC lamellar peaks can be easily rationalized from the scattering contrast differences. The neutron SLD contrast between d-PC and PCL is at least 2 orders of magnitude greater than that between the crystalline and amorphous phase for d-PC or PCL. Similarly, this contrast factor is about 1000 times greater than that between the mixed amorphous phase and the crystalline d-PC phase. Therefore, SANS is dominated by the contrast between deuterium and hydrogen or d-PC and PCL. By comparison, the electron density contrast between the crystalline and amorphous region for PCL and PC is about 160 and 30 times, respectively, greater than the corresponding neutron SLD. This difference could easily explain the strong lamellar signals observed in SAXS and their absence in SANS.

Small-Angle X-ray Scattering. The Lorentz-corrected SAXS results obtained at RT and 75 °C are shown in Figures 6 and 7, respectively. For blends with more than 50% d-PC, the SAXS profiles at RT and 75 °C are almost identical, indicating that the scattering predominantly comes from the PC lamellae. This is in agreement

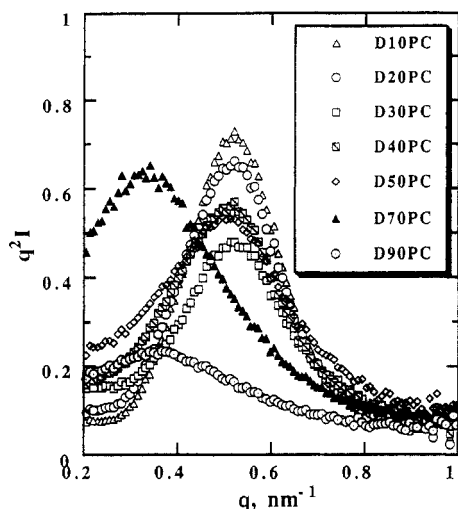


Figure 6. SAXS for d-PC/PCL blends measured at room temperature.

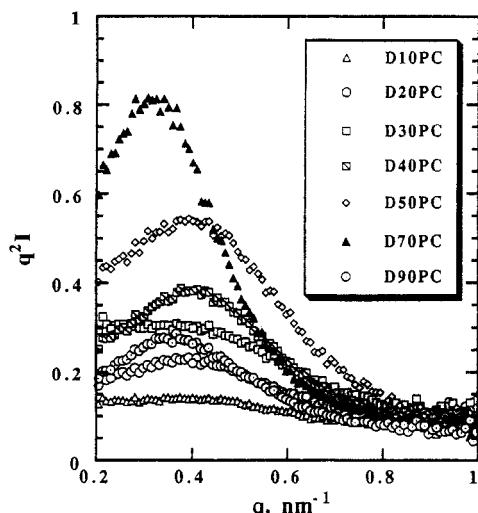


Figure 7. SAXS for d-PC/PCL blends measured at 75 °C.

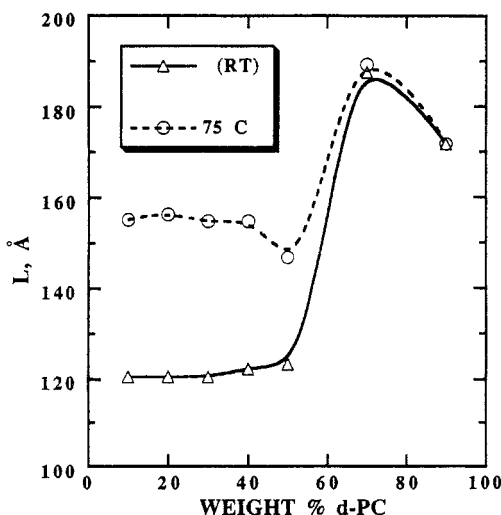


Figure 8. Long period for d-PC/PCL blends.

with the crystallization kinetics results which reveal that PCL crystallization is strongly suppressed in these materials. In general, the peaks occur at smaller q (larger long period) for the 75 °C curves as compared to those for the RT curves. These findings are summarized in Figure 8. For the PCL rich blends, the peak observed at RT is a superposition of PCL and d-PC lamellar scattering since these materials are semicrystalline/semicrystalline at

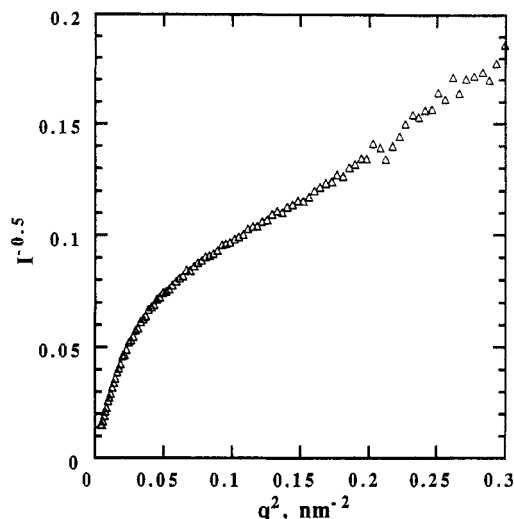


Figure 9. Debye-Bueche plot for a 50% d-PC/50% PCL blend.

temperatures below the melting point of PCL. The long periods measured from these samples represent an average size of the d-PC and PCL lamellae. This observation could suggest that the d-PC and PCL lamellae are randomly mixed, as a segregated arrangement will give rise to two peaks in the SAXS. The interpretation of the high temperature SAXS data is more straightforward since PCL is in a completely amorphous state. Figure 8 shows that the d-PC long periods in blends containing 90% to 50% PCL are almost identical. In the case of d-PC rich blends, the d-PC long period appears to increase with increasing PCL and reaches a maximum at about 30% PCL. This increase in the long period could be attributed to interlamellar incorporation of PCL in the amorphous region of the PC lamellae for the d-PC rich blends. A more quantitative analysis of the SAXS data will be explored further in a forthcoming communication.⁵

Small-Angle Neutron Scattering. As discussed before, the SANS results recorded at RT and 85 °C are almost superimposable. To simplify the analysis, the high temperature data measured from a truly two-phase material, consisting of a d-PC crystalline phase and an amorphous phase, will constitute the focus of the subsequent discussion. Classically, the Debye-Bueche model¹⁵ based on a simple exponential correlation function shown below, is normally applied to a random two-phase system.

$$\gamma(r) = \exp\left(-\frac{r}{a_c}\right) \quad (1)$$

By Fourier transforming the exponential correlation function, the intensity distribution is obtained and yields a Lorentzian function with a parameter a_c , defined as the correlation length, which is a measure of the size of heterogeneity.

$$I(q) = \frac{I(0)}{(1 + q^2 a_c^2)^2} \quad (2)$$

According to the above equation, a plot of $I^{-1/2}(q)$ versus q^2 should be linear and the [slope/intercept]^{1/2} yields a_c . Figure 9 shows a typical Debye-Bueche plot, and the deviation from linearity at small q is evident. This simple model fails to fit the SANS data over the entire q space examined in this study.

As is commonly done for a more complex system, the deviation from linearity at smaller angles is corrected for by introducing a second term to the correlation function

as shown below.

$$\gamma(r) = f \exp\left(-\frac{r}{a_1}\right) + (1-f) \exp\left(-\frac{r^2}{a_2^2}\right) \quad (3)$$

This model is often referred to as the two-correlation length model¹⁶ in which a_1 is termed the short range correlation length and a_2 is the long range correlation length. The parameter f is defined as the fractional contribution of the exponential correlation function. The intensity distribution based on the above correlation function yields a sum of a Lorentzian and a Gaussian function.

$$I(q) = \frac{A_1}{(1 + q^2 a_1^2)^2} + A_2 \exp\left(-\frac{q^2 a_2^2}{4}\right) \quad (4)$$

The parameter f , whose value ranges from 0 to 1, is defined in terms of the following equation

$$f = \frac{A_1}{A_1 + \frac{8}{\sqrt{\pi}} \left(\frac{a_1}{a_2}\right)^3 A_2} \quad (5)$$

where A_1 and A_2 are defined as below.

$$A_1 = 8\pi a_1^3 f \phi (1 - \phi) (\rho_1 - \rho_2)^2 \quad (6)$$

$$A_2 = \pi^{3/2} a_2^3 (1 - f) \phi (1 - \phi) (\rho_1 - \rho_2)^2 \quad (7)$$

The term $(\rho_1 - \rho_2)^2$ is the square of the difference of the neutron SLD between the two phases. On the basis of Table III, the SLD contrast is dominated by the contrast between d-PC and PCL. Hence, $(\rho_1 - \rho_2)$ represents the neutron SLD between these two components. The zero angle scattering is simply equal to

$$I(0) = A_1 + A_2 \quad (8)$$

Effectively, this model consists of four fitting parameters including a_1 , a_2 , A_1 , and A_2 . However, A_1 and A_2 can be calculated from eqs 6 and 7. As an internal check for the applicability of this model, the calculated zero angle scattering intensity is usually compared to the measured (curve fitted) value. It is clear that the calculated zero angle scattering depends on the parameter f which is in turn determined from the fitted values of A_1 and A_2 . Since the calculated $I(0)$ scales linearly with f , it is reasonable to assume that the parameter f has a minor contribution to the calculated $I(0)$ as compared to the higher order terms like the scattering length density contrast and the two correlation lengths.

The two-correlation length model yields a very good fit to the SANS data. A typical fit of eq 4 to the data can be found in Figure 10. The dependence of the parameter f , the fractional contribution of the exponential correlation function, and the d-PC crystallinity with composition is shown in Figure 11. Both f and d-PC crystallinity do not vary monotonically with composition. However, this complex dependence may be rationalized if a "simple-minded" correlation is made between f and d-PC crystallinity. The parameter f is a measure of the degree of exponentiality or can be regarded as a measure of "amorphousness" in the blends. This would imply that f should vary inversely with crystallinity in the blends. Furthermore, it is implicit in this reasoning that the exponential correlation function represents the amorphous component and the Gaussian correlation function describes the d-PC crystalline component. From Figure 11, one can observe that indeed the parameter f generally increases as d-PC crystallinity decreases. This relationship corroborates the assumption that the degree of exponentiality

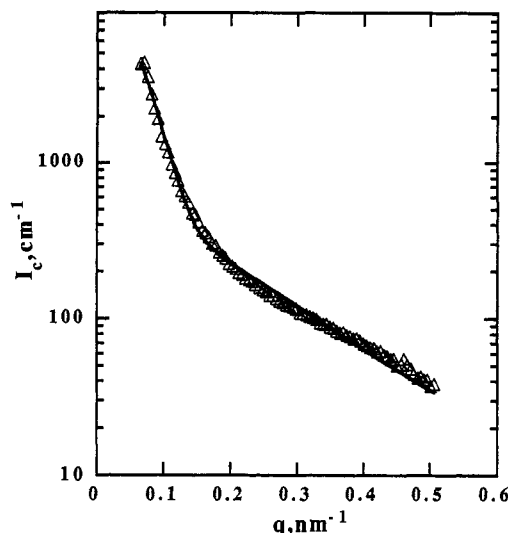


Figure 10. Two-correlation length model fit (solid line) for a 50% d-PC/50% PCL blend.

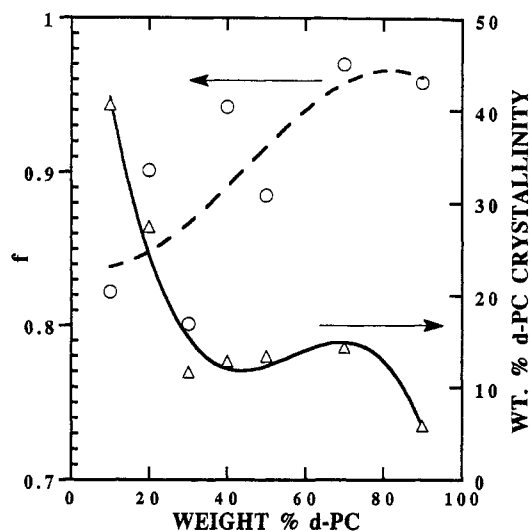


Figure 11. Normalized d-PC crystallinity and f , fractional contribution of exponential correlation function, for d-PC/PCL blends.

as expressed in terms of f is an indirect measure of the degree of "amorphousness".

The zero angle scattering intensities derived from the best fit and those calculated from eqs 6 and 7 are shown in Figure 12. The values extrapolated from the best fit and those calculated from the model agree reasonably well. Invariably, the calculated zero angle scattering intensity is always greater than that derived from the best fit. The short range and long range correlation length as a function of composition are plotted in Figure 13. On the basis of the magnitude and the composition dependence of the correlation length, one can identify the long range correlation length to be the PC crystalline domain and the short range correlation length as the correlation distance between d-PC and PCL in the amorphous phase. The long period of d-PC measured from SAXS is also plotted in this figure. Both the long range correlation length and the long period exhibit identical composition dependence and thereby further support the applicability of this two-correlation length model and our interpretation.

The long range correlation length is about 2 times larger than the long period. This discrepancy may be related to crystallization-induced phase separation where there exists a d-PC rich region, near the crystalline d-PC, within which the PCL is excluded. This picture is also consistent with

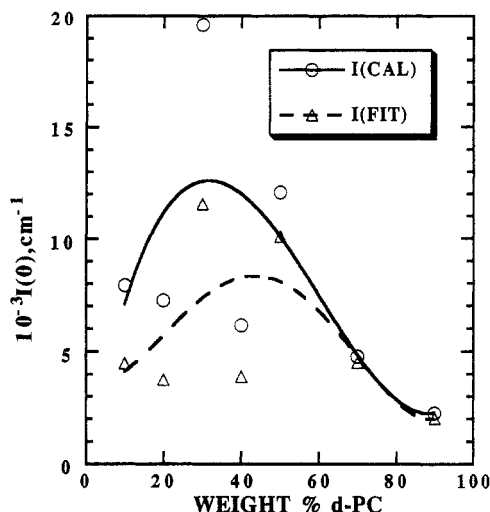


Figure 12. Zero angle scattering intensities for d-PC/PCL blends.

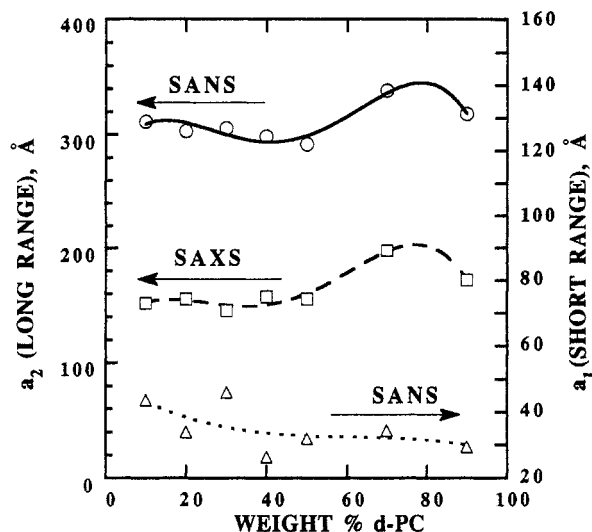


Figure 13. Long range and short range correlation lengths derived from SANS, and the long period measured from SAXS for d-PC/PCL blends.

the entropy consideration where crystalline order has to dissipate over a finite distances. It is highly entropically unfavorable to have a sharp interface between the crystalline d-PC and the amorphous phase. On the basis of this argument, the long range correlation length may be viewed as a sum of a PC crystalline domain and a PC rich phase possibly resulting from crystallization-induced localized phase separation. However, this interpretation could be one of the few possibilities. It is also important to realize that the long range correlation length does not have to be numerically equal to the long period but the two quantities are related by a proportionality constant. This statement stems directly from the fact that the correlation distance is a statistical measure whose magnitude is dependent on both the geometry and distribution of the heterogeneity.

In the theoretical framework of the Debye-Bueche model, the system is assumed to be phase separated where the size of the heterogeneity is measured by the correlation length. As stated before, the two phases in question are d-PC and PCL. On the basis of the SAXS results, the long range correlation length is attributed to the d-PC crystalline domain. By a similar argument, the short range correlation length could be related to the local cluster found in the amorphous phase. This short range order could result from localized phase separation. It is well-known that crystallization is an ordering process and could be

classified as a form of phase separation. As the blend undergoes crystallization, preferential enrichment of the crystallizing component over the other component may occur in the vicinity of the incipient crystal nuclei. These heterogeneities may develop into local clusters rich in the crystallizing component. Since thermal analytical techniques such as DSC and DMA have spatial resolution of about few hundred angstroms, these local clusters, roughly 30 Å in size, will not be detectable and the amorphous phase may still appear as homogeneous on the basis of these thermal measurements.

Summary

The semicrystalline morphologies of d-PC/PCL blends at both room temperature and elevated temperatures (above the T_m of PCL) have been examined by both SAXS and SANS. The long periods measured at RT are smaller than those obtained at elevated temperature. However, quantitative interpretation of the room temperature SAXS results is complicated by the fact that the scattering actually originates from a superposition of both PCL and d-PC lamellar scattering. For the high temperature SAXS results, the interpretation is more straightforward since PCL is completely amorphous. In the case of the semicrystalline/amorphous blends, SAXS results suggest that the d-PC lamellae remains essentially unperturbed in the PCL rich (from 90% to 50% PCL incorporation) blends. For the d-PC rich blends, the d-PC long period seems to increase with increasing PCL and shows a maximum at about 30% PCL incorporation. This complex phenomenon will be addressed in a later communication.⁵

The SANS measured at room temperature and at 85 °C are virtually identical, indicating that the scattering is dominated by the contrast between deuterium and hydrogen or d-PC and PCL. Crystalline scattering arising from PCL is negligible due the fact that crystalline/amorphous contrast is at least 2 orders of magnitude less than the d-PC and PCL contrast. A two-correlation length model yields an excellent fit to the SANS data over the entire composition range. This model reproduces not only the shape but also the absolute magnitude of the scattering curves. On the basis of the magnitude and composition dependence of the two correlation lengths, the long range correlation length is postulated to be the crystalline d-PC domain and the short range correlation length to be the local cluster in the amorphous phase. The long range correlation length is about 2 times larger than the long period measured from SAXS. This difference may be attributed to crystallization-induced localized phase separation resulting in a preferential enrichment of PC near the PC crystalline domain. In other words, the long range correlation length may be regarded as a sum of a d-PC crystalline domain and a d-PC rich phase whereas the long period represents only the d-PC crystalline domain. By a similar reasoning, the short range correlation length could be attributed to the local cluster formation, possibly resulting also from crystallization-induced phase separation. This suggests that the amorphous phase may not be truly homogeneous and exhibits clustering at about 30 Å. Since this size scale cannot be resolved by thermal analytical measurements such as DSC and DMA, the blends will still show a single glass transition temperature and the amorphous phase appears homogeneous. Therefore, combination of the SAXS and SANS results suggests a morphological model for the PCL/d-PC blends in the semicrystalline/amorphous state, composed of a d-PC crystalline phase dispersed in a matrix amorphous phase consisting of local clusters of about 30 Å in size.

Acknowledgment. Research was supported in part by the Division of Materials Sciences, U.S. Department of Energy, under Contract No. DE-AC05-84OR21400 with Martin Energy Systems Inc. and also by Novacor Inc. The authors thank P. Yazobucci of Kodak Co. for the deuterated polycarbonate synthesis and J. S. Lin of ORNL for help with the SAXS measurements.

References and Notes

- (1) Olabaisi, O.; Robeson, L. M.; Shaw, M. T. *Polymer-Polymer Miscibility*; Academic Press: New York, 1979.
- (2) Cruz, C. A.; Barlow, J. A.; Paul, D. R. *Macromolecules* **1979**, *12*, 726.
- (3) Coleman, M. M.; Zarian, J. J. *J. Polym. Sci., Polym. Phys. Ed.* **1979**, *17*, 837.
- (4) In preparation: Phase behavior and thermal stability will be discussed. Crystallization kinetics studies based on DSC, optical microscopy, and synchrotron SAXS will be reported.
- (5) In preparation: Quantitative analysis of SAXS of both semicrystalline/amorphous and semicrystalline/semicrystalline blends.
- (6) Russell, T. P.; Ito, H.; Wignall, G. D. *Macromolecules* **1988**, *21*, 1703.
- (7) Bates, F. S. *J. Appl. Crystallogr.* **1988**, *21*, 681.
- (8) Wignall, G. D.; Farrar, M.; Morris, S. *J. Mater. Sci.* **1990**, *25*, 69.
- (9) Brandrup, J.; Immergut, E. H., Eds. *Polymer Handbook*, 2nd ed.; Wiley: New York, 1975.
- (10) Khambatta, F. B.; Warner, F.; Russell, T. P.; Stein, R. S. *J. Polym. Sci., Polym. Phys. Ed.* **1976**, *14*, 1391.
- (11) Wignall, G. D.; Bates, F. S. *J. Appl. Crystallogr.* **1987**, *20*, 28.
- (12) Dubner, W. S.; Schultz, J. M.; Wignall, G. D. *J. Appl. Crystallogr.* **1990**, *23*, 469.
- (13) Wignall, G. D.; Lin, J. S.; Spooner, S. *J. Appl. Crystallogr.* **1990**, *23*, 241.
- (14) Russell, T. P.; Lin, J. S.; Spooner, S.; Wignall, G. D. *J. Appl. Crystallogr.* **1988**, *21*, 629.
- (15) Debye, P.; Anderson, H. R.; Brumberger, H. *J. Appl. Phys.* **1957**, *28*, 6.
- (16) Moritani, M.; Inoue, T.; Kawai, H. *Macromolecules* **1970**, *3* (4), 433.